

**CHAPTER IV**  
**APPLICATION OF TITANIUM DIOXIDE NANOPARTICLES**  
**IN POLYPROPYLENE NANOCOMPOSITES**

**ABSTRACT**

Titanium dioxide is an inorganic filler that is widely used in pigment and photocatalyst applications. This metal oxide has been intensively studied, especially in sub-micron or nanometer size which has attracted much interest because smaller particles have larger surface area per gram or per volume ratio and therefore can be more reactive. In this work, TiO<sub>2</sub> particles prepared via sol-gel process were introduced into polypropylene by the master batch manufacturing process and the resulting composites were compared with the blends prepared with commercial nanoparticles TiO<sub>2</sub>. The effect of TiO<sub>2</sub> contents and the characteristics of TiO<sub>2</sub> from two sources on the properties of resulting nanocomposites were studied. Results from DSC indicated that there was no change in the crystallization exotherms of composites prepared from TiO<sub>2</sub> by sol-gel process whereas the composites prepared with commercial nano-TiO<sub>2</sub>, the added TiO<sub>2</sub> acted as a nucleating agent. At 5wt% and 10wt% of TiO<sub>2</sub> in polypropylene were able to shift the crystallization exotherms by 6°C and 8°C, respectively, and therefore resulted in higher degree of crystallinity as observed from DSC and XRD. TiO<sub>2</sub> particles from sol-gel process were still in micro size whereas the commercial TiO<sub>2</sub> were much smaller, therefore it had more effect on the properties of polymer. Thermogravimetric analysis results showed that the degradation temperature of composites prepared from both sources of TiO<sub>2</sub> was increased by increasing contents of TiO<sub>2</sub>, suggesting that the addition of nano-TiO<sub>2</sub> can improve the thermal stability of polymer. At 1-5wt% of TiO<sub>2</sub> from two sources in PP, there were no adverse effects on mechanical properties of the composites, whereas at 10wt% commercial TiO<sub>2</sub>, it can increase much in Young's modulus due to higher in degree of crystallinity in this content.

**(Key-words:** Titanium Dioxide, Nanoparticles, Polypropylene, Masterbatch Manufacturing Process, Crystallization, Thermal Stability, Mechanical Properties)

## INTRODUCTION

Nanotechnology is one of the key technologies of this century and nanoparticles inorganic filler have been intensively studied such as Si, Al, Ti and Zn. In this work we will concentrate on Titanium (Ti), this element is finding more and more applications in today's society. Over 90% of the worldwide use of titanium is in the oxide form,  $\text{TiO}_2$  (Titanium Dioxide), thus creating a high demand. With "little effect" and "surface effect" the nanoparticle has many special properties that are different from those of other larger particles [1] because smaller particles have larger surface area per gram or per volume ratio and therefore can be more reactive.

Modification of the polymer with inorganic nanoparticles results in polymer/inorganic nanoparticle composites with excellent performance due to the combination of higher hardness, durability and thermal stability of the inorganic filler and the good flexibility, toughness and processability of the polymer [2-6]. Nanoparticle filled polymers exhibit enhanced mechanical, thermal, electrical, optical, and barrier properties at rather low nanoparticle loadings compared to traditional composites [1, 7, 8, 9]. However, in the process of preparation, there are the great number of factors affecting the properties of the resultant polymer/inorganic nanoparticle composites [10-12]. The main factors are the nanoparticle size and volume (or weight) fraction, the nature of the matrix and its adhesion to the nanoparticle, the nanoparticle dispersing into the matrix, and manufacturing technology. Among these factors, the interfacial adhesion and dispersing are of cardinal importance and markedly influence the properties of nanoparticle-filled polymers.

In this present work, attempts to "disperse" of  $\text{TiO}_2$  nanoparticles and polymer using master batch manufacturing process.  $\text{TiO}_2$  particles were from two sources, the first was commercial grade and the other was synthesized via sol-gel process using starting material Titanium diisopropoxide bis (acetylacetonate) 75wt% solution in 2-propanol and Triol (Pentaerythritol) as a linking agent. The effect of particle size from two sources of  $\text{TiO}_2$  and the effect of  $\text{TiO}_2$  content on the properties of resulting composites were studied. Isotactic Polypropylene were chosen as a polymer matrix, it is a commodity plastic, cheap, good strength and easily

process. Attention was focused on crystallization, crystalline structure, thermal stability, mechanical properties and morphology of the obtained composites.

## EXPERIMENTAL DETAILS

### Materials

Polypropylene used in this work was produced and supplied by HMC Polymers Company Limited. Some physical properties of the resin, reported by the manufacturer, are melt flow rate = 22 dg/min (ASTM D1238), density = 0.90 g/cm<sup>3</sup> (ASTM D792B), tensile strength at yield = 34 Mpa (ASTM D638), elongation at yield = 9% (ASTM D638), flexural modulus = 1480 Mpa (ASTM D790A), notched izod impact strength = 22 J/m (ASTM D256A), and deflection temperature = 97 °C (ASTM D648).

TiO<sub>2</sub> particles from two sources were used, the first was commercial grade supplied by JJ-Degussa Thailand and the other was synthesized via sol-gel. TiO<sub>2</sub> particles prepared via sol-gel method using starting materials titanium diisopropoxide bis(acetylacetonate) 75 wt% solution in 2-propanol and tetraol (Pentaerythritol) as a linking agent, the reaction was carried out at 70°C for 3 hours. The mole ratio between Titanium diisopropoxide bis(acetylacetonate) and tetraol was 2:1. After the reaction was completed, the titanium sol was obtained. Then HCl and H<sub>2</sub>O (1:10) were added and heated at 70°C until they were homogeneous to obtain the optimized colloidal sol. The size of the sol was characterized by shining a laser light through the solution. Results from the test indicated that the size of the obtained sol was in the range of nanometer. The obtained sol was dried under vacuum and was ground before calcination. Finally, the dried titanium compound (dried gel) was calcined at 650°C for 3 hours to remove any remaining organic residues to obtain TiO<sub>2</sub> particles. Both sources of TiO<sub>2</sub> were observed to be the anatase structure by XRD.

The surface area, pore volume and pore size of the two sources of TiO<sub>2</sub> were characterized using BET (autosorp one). The surface area, pore volume, and pore size of commercial TiO<sub>2</sub> were 56.9m<sup>2</sup>/g, 1.84 x 10<sup>-2</sup>cc/g, and 12.9 nm, respectively and the surface area, pore volume, and pore size of synthesized TiO<sub>2</sub>

were  $3.31\text{m}^2/\text{g}$ ,  $2.02 \times 10^{-2} \text{cc}/\text{g}$ , and  $24.4 \text{ nm}$ , respectively. The average particle size of  $\text{TiO}_2$  was measured by a Malvern (Masterizer X). The average particle size (D [4,3]) of commercial  $\text{TiO}_2$  was  $2.95 \mu\text{m}$  and synthesized  $\text{TiO}_2$  was  $72.95 \mu\text{m}$ . It should be noted that the particle size that observed from this equipment was the agglomerate size.

### **Nanocomposites Preparation**

PP and  $\text{TiO}_2$  nanoparticles were dried at  $60^\circ\text{C}$  for 4 hours before melt compounding. The master batch of 10 wt%  $\text{TiO}_2$  was prepared by using a Collin ZK25 self-wiping, co-rotating twin-screw extruder with screw speed 50 rpm. The as-prepared master batch was blended with the required amount of PP to give 1, 2, 3, 4, and 5 wt% of  $\text{TiO}_2$  in PP. For  $\text{TiO}_2$  from sol-gel process, due to the small amount of  $\text{TiO}_2$  prepared, only 5wt% of  $\text{TiO}_2$  in PP master batch was prepared. Then the as-prepared master batch was blended with the required amount of PP to give 1 and 3 wt% of  $\text{TiO}_2$  of PP composites.

### **Specimen Preparation**

A film of each sample was prepared from compression-molded sheet with a V50H compression press (Wabash). The obtained pellets were placed between a pair of stainless steel platens, and the mold was preheated at  $200^\circ\text{C}$  for 5 min between the plates without any applied pressure to allow complete melting. After that the mold was compressed under a force of 10 tons with a residence time of 5 min and this specimen was cooled at  $50^\circ\text{C}$  under pressure. Each film specimen was used for studying non-isothermal crystallization and subsequent melting behavior.

An ARBURG Allrounder 270M injection molding machine was used to prepare specimens for mechanical tests. The operating settings of the machine were as follow; barrel temperature =  $190^\circ\text{C}$ , nozzle temperature =  $200^\circ\text{C}$ , clamping force = 25 kN, and injection pressure = 1000 bar. Tensile specimens were prepared according to ASTM D638-91 standard test method.

### **Differential Scanning Calorimetry**

Non-isothermal melt-crystallization and the subsequent melting behavior of neat polymer PP and PP filled with various contents of TiO<sub>2</sub> were investigated on a Perkin-Elmer Series 7 differential scanning calorimeter (DSC). A temperature calibration was performed on every other run using a pure indium standard ( $T_m = 156.6^\circ\text{C}$  and  $\Delta H_f = 28.45 \text{ J.g}^{-1}$ ). A sample of  $5.0 \pm 1.0 \text{ mg}$  in weight, was sealed in an aluminium sample holder. The experimental procedure started with heating each sample from 50 to  $250^\circ\text{C}$  at a heating rate of  $10^\circ\text{C.min}^{-1}$  in order to set a similar thermal history for all the samples studied. To ensure complete melting, the sample was kept at  $250^\circ\text{C}$  for a holding period of 5 min, after which each sample was cooled down at a cooling rate of  $10^\circ\text{C.min}^{-1}$  to  $50^\circ\text{C}$  in order to observe non-isothermal melt crystallization behavior. As soon as the program temperature reached  $50^\circ\text{C}$ , the sample was immediately reheated at a heating rate of  $10^\circ\text{C.min}^{-1}$  to  $250^\circ\text{C}$  in order to observe the subsequent melting behavior. Both the non-isothermal melt-crystallization exotherm and subsequent melting endotherm were recorded for further analysis.

### **Wide Angle X-ray Diffractometer**

A Rigaku Rint 2000 wide-angle X-ray diffractometer (WAXD) was used to determine the crystal structure and degree of crystallinity of all composites which were non-isothermally melt-crystallized at a cooling rate of  $10^\circ\text{C.min}^{-1}$  in DSC. Wide angle X-ray diffractometer equipped with a graphite monochromator and a Cu tube for generating CuK $\alpha$  radiation ( $1.5046 \text{ \AA}$ ). The samples were examined between  $5^\circ$ - $90^\circ$   $2\theta$  at a scanning rate of  $5^\circ 2\theta/\text{min}$  in  $0.02^\circ 2\theta$  increments. CuK $\alpha$  radiation with  $\lambda = 0.514 \text{ nm}$  was used as the X-ray source, operated at 40 kV and 30 mA. The digital output of the proportional X-ray detector and goniometric angle measurements were sent to an online micro computer for storing the data. Percent crystallinity was calculated using Crystallinity Multipeak Method.



### **Dynamic Mechanical Analysis**

Dynamic mechanical of these composites were studied using a Solid Analyzer RSA II (Rheometric scientific). The storage modulus ( $E'$ ) and loss modulus ( $E''$ ) were measured as a function of temperature. The three point bend fixture was used to mount the samples and temperature step of 4K intervals. All experiments were performed at 1Hz frequency and 0.025% strain amplitude using static force tracing dynamic force.

### **Thermogravimetric Analysis**

Thermogravimetric and derivative thermogravimetric tests were carried out using TG-DTA analyzer. The experiment was done at a temperature in the range of 30-600°C under ambient atmosphere. The values of degradation temperatures were reported.

### **Mechanical Property Measurements**

Tensile tests were performed with an Instron Universal testing machine, Model 4206, at room temperature following the procedure describe in ASTM D638-91. A crosshead speed of 40 mm.min<sup>-1</sup> and 100 kN load cell was used for all measurements. The value of tensile strength at yield, percentage of elongation at yield and Young's modulus for all composites were investigated. The results from the tests were reported as an average of the data taken from 5 specimens.

### **Morphological Observation**

Energy dispersive X-ray spectrometer (EDS), OXFORD (link ISIS series 300) composition distribution map was used to analyze and confirm Ti element in composites. Scanning electron microscope (SEM), JEOL (JSM-6400) was used to observe the dispersion of TiO<sub>2</sub> of the fractured surface of selected specimens which were fractured in liquid nitrogen and also use to measure particle size of TiO<sub>2</sub> in composites. The samples were sputtered with gold before viewing under a scanning electron microscopy (SEM) operating at 15 kV.

## RESULTS AND DISCUSSION

### Differential Scanning Calorimetry

Figure 4.1 and 4.2 illustrates non isothermal melt crystallization exotherms, recorded at a cooling rate of 10°C/min for neat PP and PP filled with various contents of TiO<sub>2</sub>. For non isothermal melt crystallization, it was shown that the melt crystallization temperature of PP was increased by increasing the contents of commercial TiO<sub>2</sub>. The temperature was shifted by 6°C and 8°C when the weight contents of commercial TiO<sub>2</sub> were increased from 5% to 10% (see Figure 4.1). For composites prepared from synthesized TiO<sub>2</sub>, there was no change in melt crystallization temperature even at 5wt% of TiO<sub>2</sub> (see Figure 4.2), this observation might conclude that commercial TiO<sub>2</sub> acted as a nucleating agent for isotactic polypropylene [13], whereas the synthesized one could not. The reason for these results derive from the differences in particle size and also surface area of two sources of TiO<sub>2</sub>. From the agglomerate particle size as reported, the synthesized TiO<sub>2</sub> was much larger in size (72.95 μm) and had much smaller surface area (3.31 m<sup>2</sup>/g) compared to the commercial TiO<sub>2</sub> which was much smaller in size (2.95 μm) and had larger surface area (56.9 m<sup>2</sup>/g). Therefore commercial TiO<sub>2</sub> has better ability to be a nucleating agent than the synthesized one.

For the melting endotherms, the addition of both commercial and synthesized TiO<sub>2</sub> to PP composites did not have any effect on melting temperature and also melting peak pattern as shown in Figure 4.3, 4.4 and Table 4.1, 4.2. The values of melting enthalpy ( $\Delta H_m$ ) of neat PP and PP with various contents of TiO<sub>2</sub>, obtained via DSC are also presented in Table 4.3. The values of melting enthalpy ( $\Delta H_m$ ) of PP tended to increase by increasing the contents of commercial TiO<sub>2</sub> especially at 10wt% of TiO<sub>2</sub>, the  $\Delta H_m$  was the highest at 101.16 J/g. The value of this parameter, indicating the crystallinity of a polymer [14], increases as the TiO<sub>2</sub> contents increase.

### Wide Angle X-ray Diffractometer

In order to observe the crystal structure and the resulting apparent degree of crystallinity of neat PP and PP composites investigated, WAXD technique was utilized. Figure 4.5 illustrates WAXD pattern for neat PP and PP filled with various contents of commercial TiO<sub>2</sub>. It should be noted that the samples were prepared in the DSC cell by cooling at a rate of 10°C/min after melt annealing at 250°C for 5 minutes. For isotactic polypropylene, the characteristic X-ray peaks were observed at the scattering angles  $2\theta$  of ca. 14.1°, 16.9°, 18.6°, 21.2° and 21.9° which are  $\alpha$ -phase, corresponding to the reflection planes of (110), (040), (130), (111) and (041), respectively [15]. The results shown in Figure 4.5 can be seen that addition of commercial TiO<sub>2</sub> at 1-3 weight percent did not alter the peak pattern of PP. The peak pattern of PP was changed at 4, 5 and 10 weight percent of commercial TiO<sub>2</sub> composites, it was assumed that the peak at  $2\theta = 16.9^\circ$  of PP may shifted to  $2\theta$  around 15.9° and the peak at  $2\theta$  around 16.9° come from the  $\beta$ -phase of nucleating agent or  $\beta$ -nucleator [16], as already discussed earlier that TiO<sub>2</sub> acted as nucleating agent and the intensity at  $2\theta = 16.9^\circ$  was seemed to increase by increasing the weight contents of commercial TiO<sub>2</sub> from 4 to 10%. The degree of crystallinity of composites investigated from Crystallinity Multipeak Method was summarized in Table 4.3, the values tended to increase by increasing weight contents of commercial TiO<sub>2</sub> which corresponded to the DSC results. For synthesized TiO<sub>2</sub>, the peak pattern was not changed with any contents of TiO<sub>2</sub> as shown in Figure 4.6.

### Dynamic Mechanical Analysis

Results from DSC and XRD showed that the degree of crystallinity was higher when increasing TiO<sub>2</sub> contents, it would be expected that  $T_g$  of the PP composites should be higher because the inorganic particles should hinder segmental motions of the polymer chains. From DMA plots of loss modulus ( $E''$ ) against temperature to determine  $T_g$  of different composites obtained (see Figure 4.9). The composites prepared from 1-5wt% commercial TiO<sub>2</sub> did not show any significant effect on  $T_g$  of polypropylene. However, at 10wt% of commercial TiO<sub>2</sub> composite, it showed slight decreased in  $T_g$  to a lower temperature (0.38°C) when compared to the



neat PP (4.56°C). As polypropylene is the semi-crystalline polymer, therefore it is not only the crystalline part that is important but also the amorphous region which also has an effect on characteristics of polymer chains. However it was anticipated that at high contents of TiO<sub>2</sub>, the possibility of TiO<sub>2</sub> particles to move to the amorphous part was higher as well therefore the steric hindrance presented by the TiO<sub>2</sub> particles toward the more difficult interaction between polymer chains in amorphous region can be occurred and resulted in lower T<sub>g</sub>. As synthesized TiO<sub>2</sub> did not have an effect on T<sub>g</sub> of polypropylene with the load of TiO<sub>2</sub> added as shown in Figure 4.10.

#### **Thermogravimetric Analysis**

TGA was used to determine the degradation temperature of the nanocomposites obtained. The degradation temperature of nanocomposites was found to increase by increasing contents of both commercial and synthesized TiO<sub>2</sub>. The highest degradation temperature (T<sub>d</sub>) was observed at nanocomposites prepared from 5 weight percent of commercial TiO<sub>2</sub> which was 378.9 °C compared to neat PP which was just 342.4°C. The addition of 5wt% of synthesized TiO<sub>2</sub> can also increase the degradation temperature of composites to 360.4°C (see Figure 4.11).

#### **Tensile Property Measurements**

The tensile strength at yield, percentage of elongation at yield and Young's modulus of all composites were investigated. The tensile strength of 1-5wt% commercial TiO<sub>2</sub> filled composites were little different from those of the neat PP. However, at 10wt% of TiO<sub>2</sub> in composite resulted in large reduction of tensile strength as shown in Figure 4.12. These results would suggest that it is due to the higher degree of crystallinity of nanocomposites. When it was pulling, the order structure or crystalline structure was alter and could not repack to the tensile direction therefore it could not be pulled any further and would then break with lower strength. The other reason which can make the tensile strength reduce may come from the orientation of crystals in polymer chain. They distributed unevenly like many spots in chain (TiO<sub>2</sub> acted as nucleating agent) and the spots could not

help the orientation in the tensile direction. The percentage of elongation was reduced by increasing the weight contents of commercial  $\text{TiO}_2$  (see Figure 4.13). The Young's modulus were seemed to increase at 5wt% commercial  $\text{TiO}_2$  and from the graph, it was clearly indicated that there was a large increase in Young's modulus at 10wt% commercial  $\text{TiO}_2$ , as compared to 0-4wt% of composites (see Figure 4.14), suggesting that owing to higher crystallinity at 5 and 10wt% of  $\text{TiO}_2$  that made the increasing of modulus. The PP composites with the synthesized  $\text{TiO}_2$  (1, 3 and 5wt%) did not affect on tensile strength and Young's modulus of composites but the percentage of elongation was reduced by increasing weight content of the synthesized of  $\text{TiO}_2$  but the reduction was still lower when compared to the composites prepared from commercial  $\text{TiO}_2$  (see Figure 4.15-4.17).

### Scanning Electron Microscope

Energy dispersive X-ray spectrometer was used to locate Titanium element as labeled in the images. SEM micrographs of the fractured surface of PP filled with 5 and 10 wt% of commercial  $\text{TiO}_2$  are illustrated in Figure 4.18. The contents of  $\text{TiO}_2$  that were lower than 5wt% were not observed, due to the very small amount of the  $\text{TiO}_2$  added. The image obtained from composites with 5wt% commercial  $\text{TiO}_2$  showed that the  $\text{TiO}_2$  particles were still in nanometer range, whereas the composites prepared from 10wt% was in micrometer, this may be due to the agglomeration of  $\text{TiO}_2$  particles. The pore volume of commercial  $\text{TiO}_2$  was 10 times larger than the synthesized one so it looked like much more content than the synthesized one when considering in same weight, therefore the probability to agglomerate was much easier. Although the agglomeration occurred but at 10wt% still had many effects on the properties of polymer as already discussed.

### CONCLUSIONS

In this work,  $\text{TiO}_2$  particles prepared via sol-gel process were introduced into polypropylene by the master batch manufacturing process. The resulting composites were compared with the blends prepared with commercial nanoparticles  $\text{TiO}_2$ . The effect of  $\text{TiO}_2$  contents and the properties of  $\text{TiO}_2$  from two sources of  $\text{TiO}_2$  on the properties of resulting nanocomposites were studied. Results from DSC

indicated that there was no change in the crystallization exotherms of  $\text{TiO}_2$  from sol-gel process whereas composites with commercial nano- $\text{TiO}_2$ , the added  $\text{TiO}_2$  acted as a nucleating agent. At 5wt% and 10wt% of  $\text{TiO}_2$  in polypropylene being able to shift the crystallization exotherms by  $6^\circ\text{C}$  and  $8^\circ\text{C}$ , respectively, and therefore the commercial  $\text{TiO}_2$  can increase the degree of crystallinity of nanocomposites by increasing weight contents of  $\text{TiO}_2$  as observed from DSC and XRD.  $\text{TiO}_2$  particles from sol-gel process were still in micro size whereas the commercial  $\text{TiO}_2$  were much smaller, therefore it had more effect on the properties of polymer. Thermogravimetric analysis results showed that degradation temperature of composites was increased by increasing contents of nano- $\text{TiO}_2$  from two sources, suggesting that the addition of nano- $\text{TiO}_2$  can improve the thermal stability of polymer. At 1-5wt% of  $\text{TiO}_2$  from two sources in PP, there were no adverse effects on mechanical properties of the composites, whereas at 10wt% commercial  $\text{TiO}_2$  can increase much in Young's modulus due to higher in degree of crystallinity in this content.

The advantage of synthesis  $\text{TiO}_2$  in sol-gel tetraol based method is the starting materials are stable in room temperature and the condition during the reaction is mild, but the obtained nanoparticles were agglomerated after calcination at high temperature. The grinding process after calcination cannot control the size of particles as expected. The author would like to suggest the improvement of synthesis of  $\text{TiO}_2$  to be of smaller particles in order to have larger surface area. The first method is to try reducing the calcined temperature of  $\text{TiO}_2$  to prevent the particles coming to agglomerate, but still need to make sure that it can also remove the organic substance from the compound and after calcination the particles should be sonicated in the solution instead of grinding. The other way is to find some coating compounds such as Hydroxypropyl cellulose [17] and Carboxymethyl cellulose to prevent the agglomeration of  $\text{TiO}_2$  particles.

#### **ACKNOWLEDGEMENTS**

Authors are thankful to HMC Polymer, JJ Degussa (Thailand), for providing the materials for carrying out the present work.

**REFERENCES**

1. Zhang, J., Wang, X., Lu, L., Yang, X., *J Appl Polym Sci* 2003, 87, 381.
2. Grocela, T.A., Nauman, E.B., *Polymer* 1993, 34, 2315.
3. Gleiter, H., *Adv Mater* 1992, 4, 474.
4. Novak, B.M. *Adv Mater* 1993, 5, 422.
5. Komarmaeni, S., *J Mater Chem* 1992, 2, 1219.
6. Kornmann, X., Berglung, L.A., Sterte, J., Glannelis, E.P., *J Polym Eng Sci* 1998, 8, 1351.
7. Wu, C.S., *J Appl Polym Sci*, 2004, 92, 1749.
8. Xiao, Y., Wang, X., Yang, X., Lu, L., *Mater Chem Phys* 2002, 77, 609.
9. Liu, Y., Jim, Y., Hong, L., *J Appl Polym Sci* 2003, 89, 2815.
10. Calvert, P., Burdon, J. *Polym Mater Sci Eng* 1994, 70, 224.
11. Karokawa, Y., Yasuda, H.J., *Mater Sci Lett* 1996, 15, 1481.
12. Sumita, M., Tsukumo, Y. *J Mater Sci* 1993, 18, 1758.
13. Supaphol, P., Charoenphol, P., and Junkasem, J., *Macro Mater Eng* 2004, 289, 818.
14. Liao, H.T., Wu, C.S., *J Polym Sci Part B : Polymer Physics* 2004, 42, 4272.
15. Florencio, G.m Tomas Jeferson, A., Marcelo, S., *Polymer Degradation and Stability* 2005, 89, 383.
16. Liu, S. L., Lim, S.H., Zhao, J. H., Juay, Y. K., *SIMTech Technical reports* 2005, 6, 33.
17. Ki, D.K., Tae, J.L., Hee, T.K., *Colloid and Surface* 2003, 224, 1.

**Figure 4.1** Non isothermal melt crystallization exotherms for neat PP and PP with different amounts of commercial TiO<sub>2</sub>: (a) neat PP, (b) 1wt% TiO<sub>2</sub>, (c) 2wt% TiO<sub>2</sub>, (d) 3wt% TiO<sub>2</sub>, (e) 4wt% TiO<sub>2</sub>, (f) 5wt% TiO<sub>2</sub>, and (g) 10wt% TiO<sub>2</sub>.

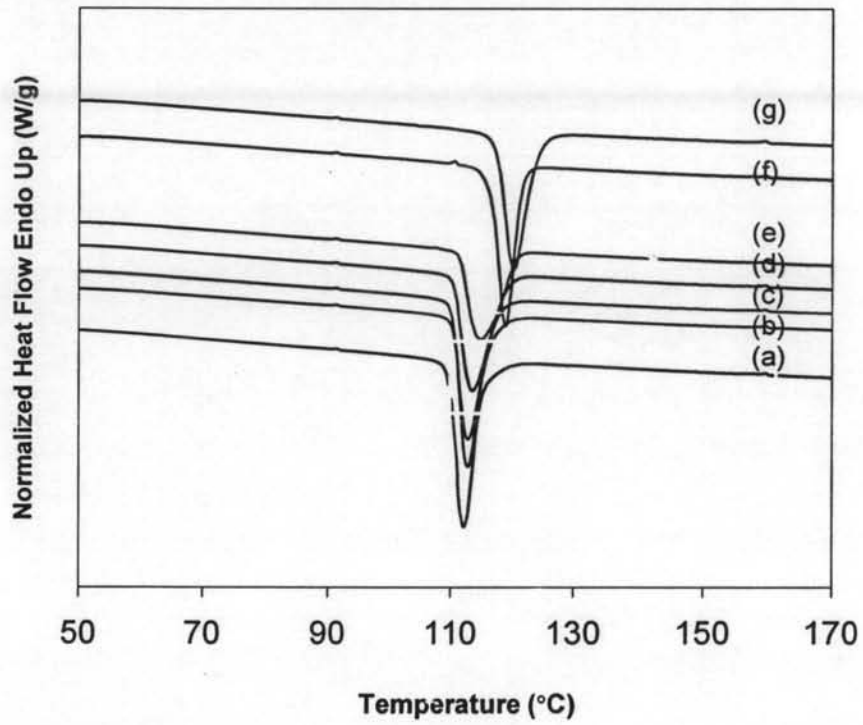




**Figure 4.2** Non isothermal melt crystallization exotherms for neat PP and PP with different amounts of synthesized TiO<sub>2</sub>: (a) neat PP, (b) 1wt% TiO<sub>2</sub>, (c) 3wt% TiO<sub>2</sub>, and (d) 5wt% TiO<sub>2</sub>.

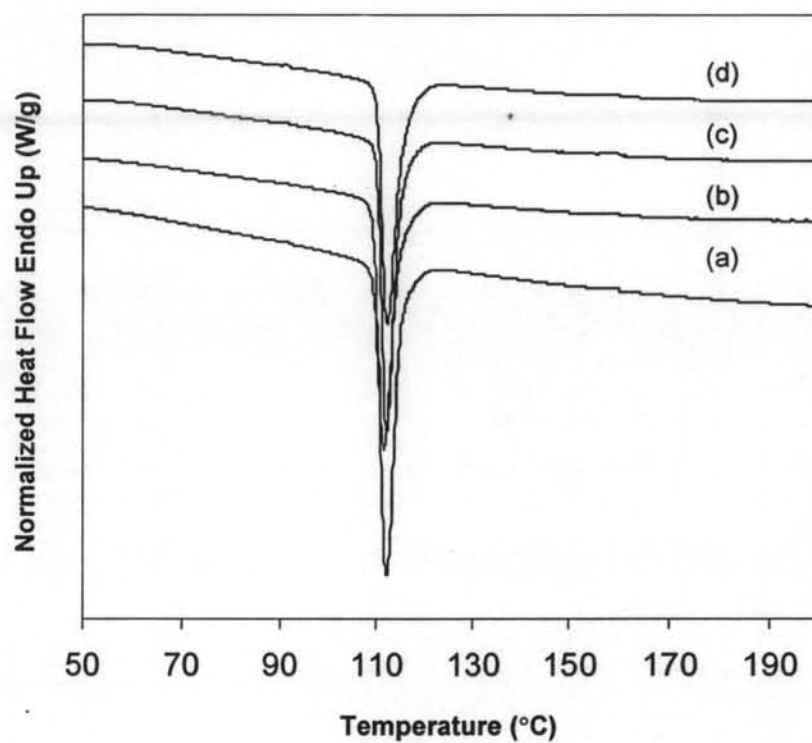


**Figure 4.3** Subsequent melting endotherms for neat PP and PP with different amounts of commercial  $\text{TiO}_2$ : (a) neat PP, (b) 1wt%  $\text{TiO}_2$ , (c) 2wt%  $\text{TiO}_2$ , (d) 3wt%  $\text{TiO}_2$ , (e) 4wt%  $\text{TiO}_2$ , (f) 5wt%  $\text{TiO}_2$ , and (g) 10wt%  $\text{TiO}_2$ .

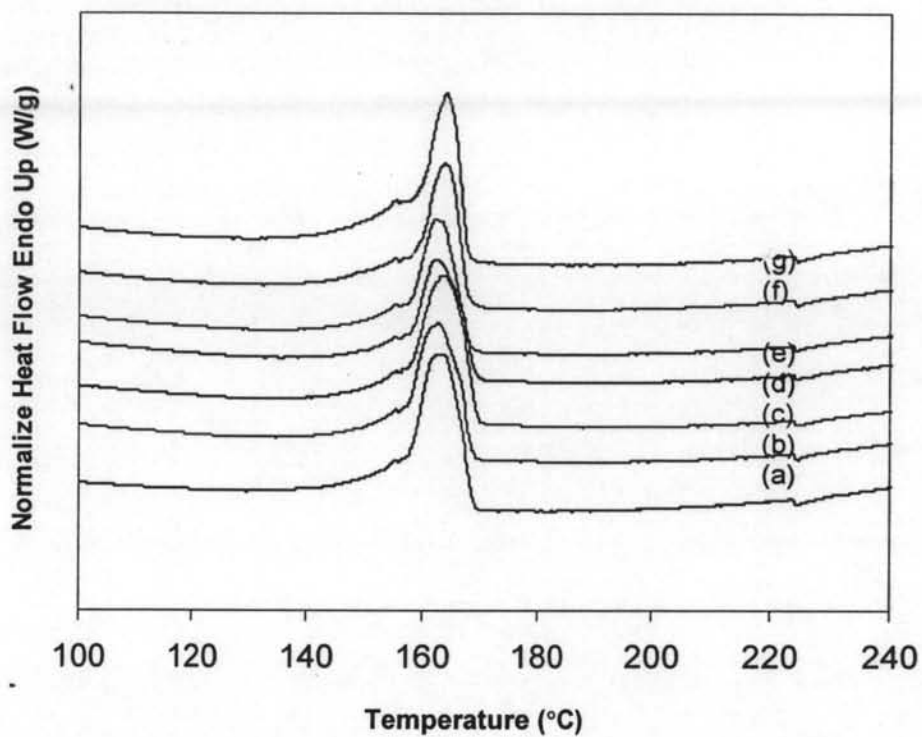


**Figure 4.4** Subsequent melting endotherms for neat PP and PP with different amounts of synthesized  $\text{TiO}_2$ : (a) neat PP, (b) 1wt%  $\text{TiO}_2$ , (c) 3wt%  $\text{TiO}_2$ , and (d) 5wt%  $\text{TiO}_2$ .

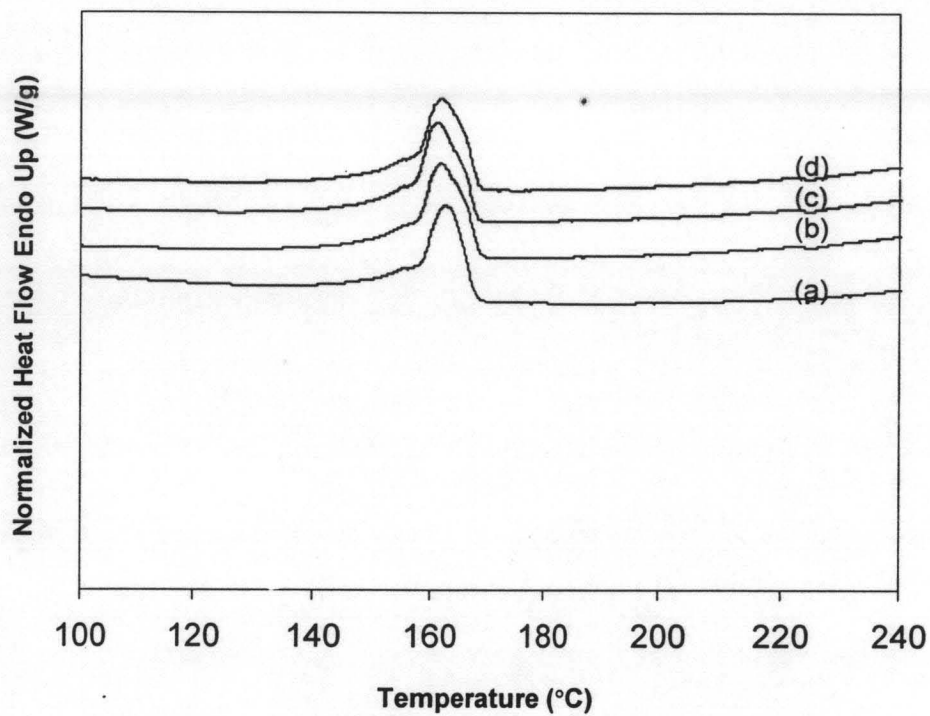


**Figure 4.5** WAXD patterns for neat PP and PP filled with different amounts of commercial TiO<sub>2</sub>: (a) neat PP, (b) 1wt% TiO<sub>2</sub>, (c) 2wt% TiO<sub>2</sub>, (d) 3wt% TiO<sub>2</sub>, (e) 4wt% TiO<sub>2</sub>, (f) 5wt% TiO<sub>2</sub>, and (g) 10wt% TiO<sub>2</sub>.

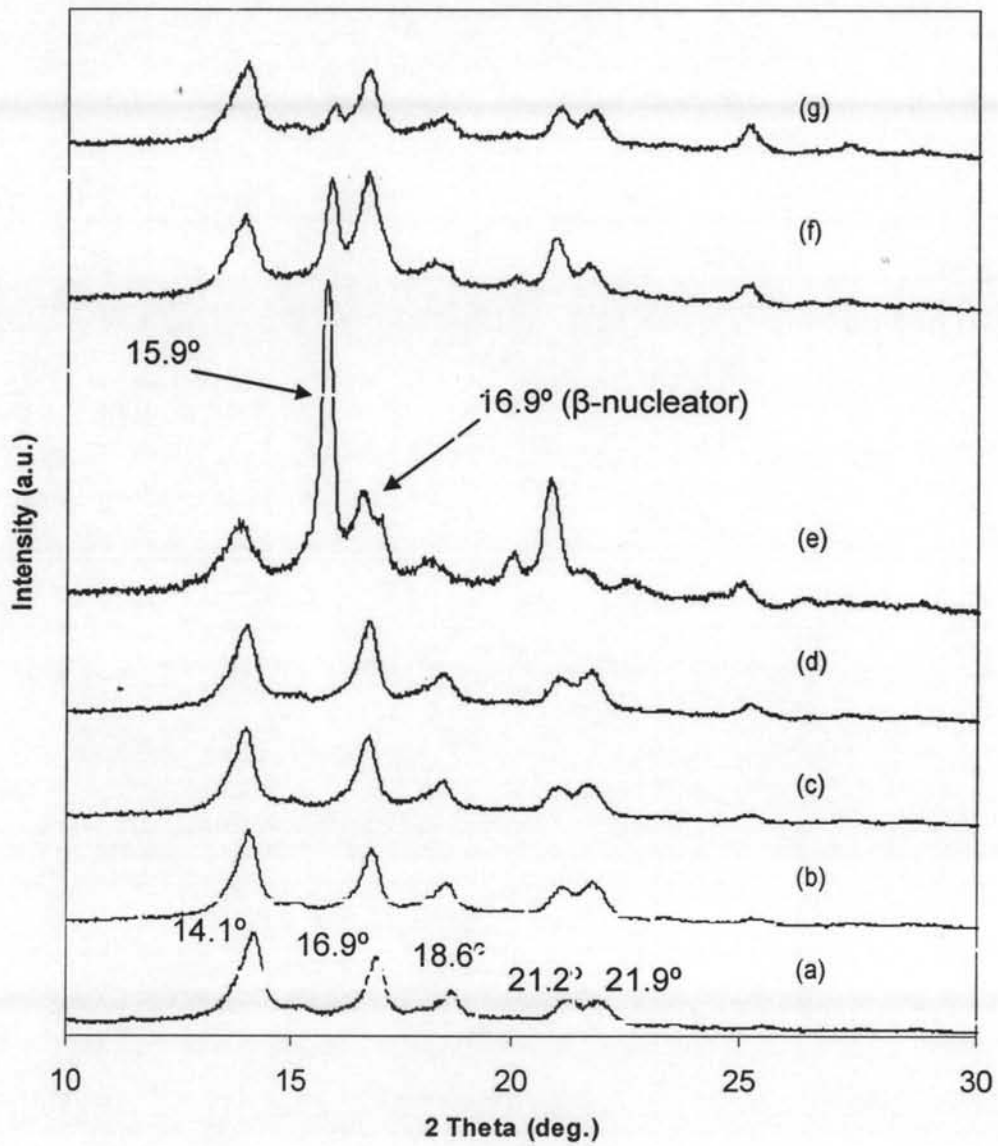


**Figure 4.6** WAXD patterns for neat PP and PP filled with different amounts of synthesized TiO<sub>2</sub>: (a) neat PP, (b) 1wt% TiO<sub>2</sub>, (c) 3wt% TiO<sub>2</sub>, and (d) 5wt% TiO<sub>2</sub>.

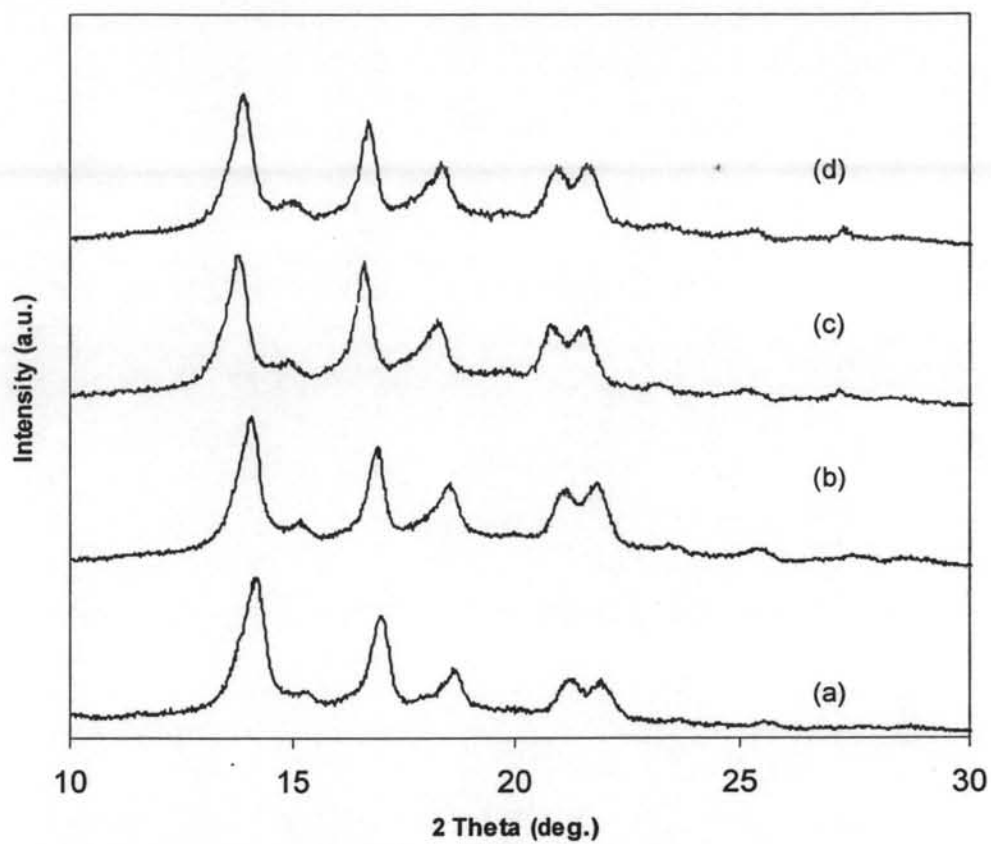
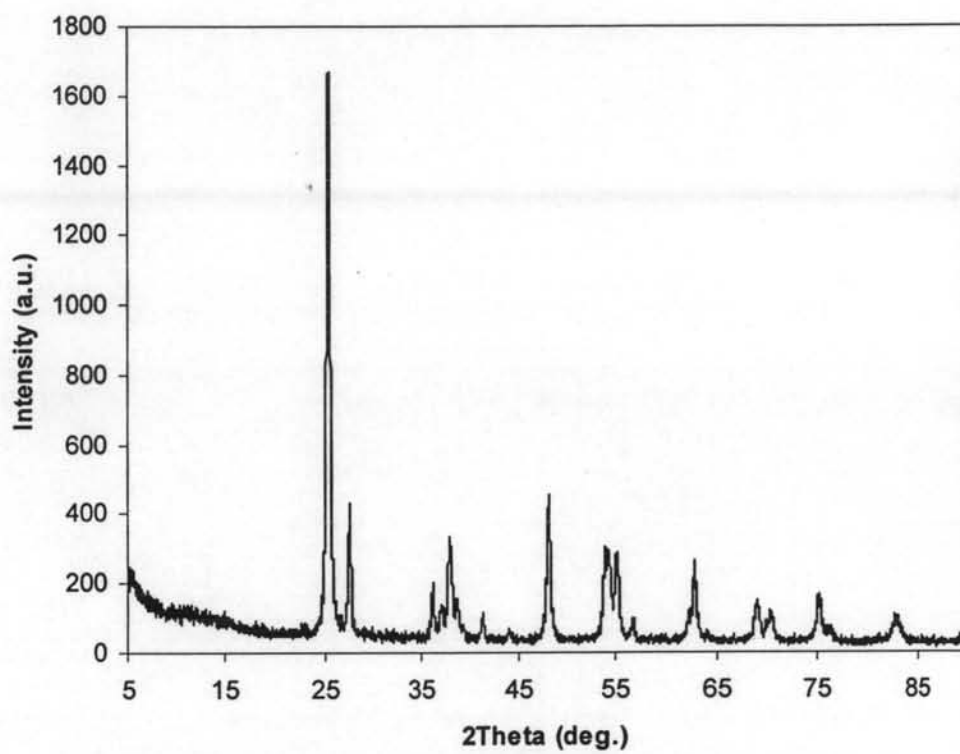




Figure 4.7 WAXD patterns of commercial  $\text{TiO}_2$ .



**Figure 4.8** WAXD patterns of synthesized  $\text{TiO}_2$ .

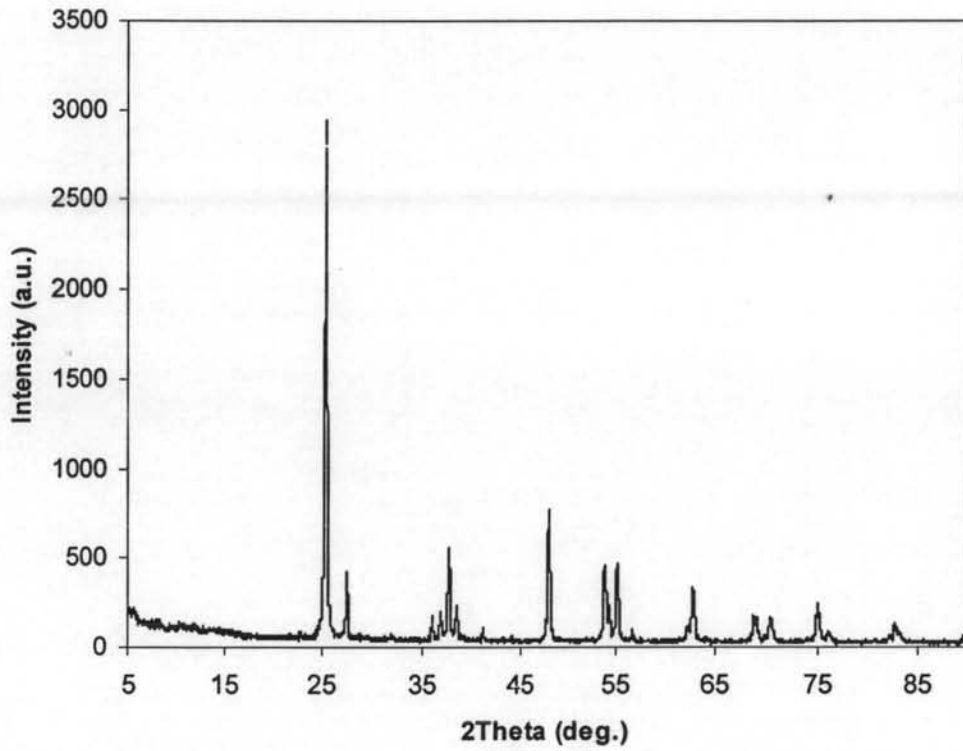


Figure 4.9 DMA results for neat PP and PP filled with different amounts of commercial  $\text{TiO}_2$ .

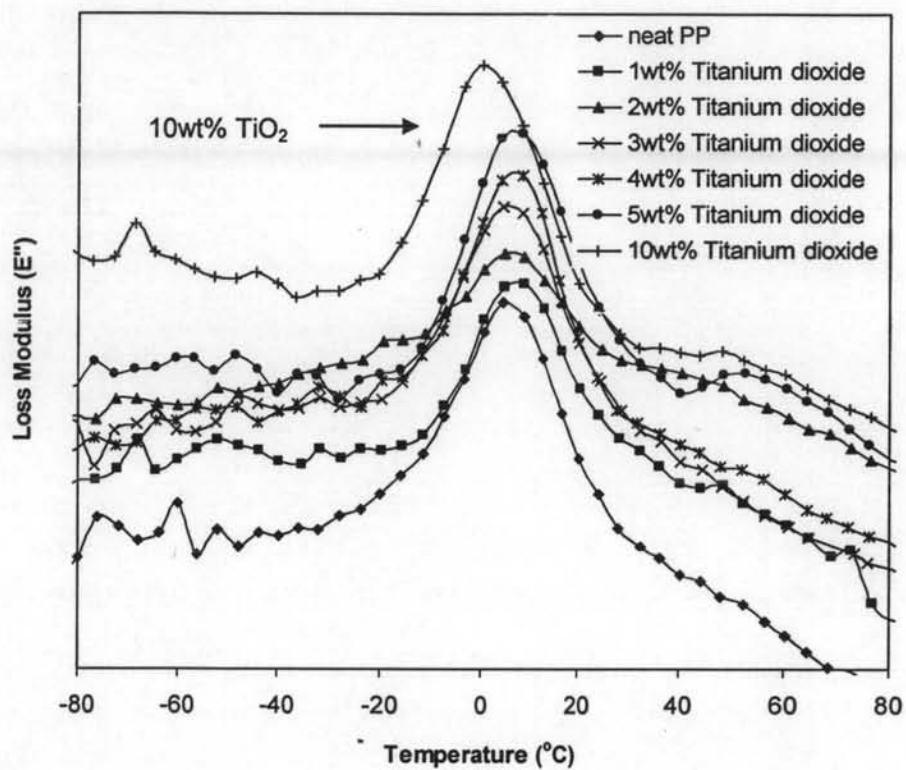


Figure 4.10 DMA results for neat PP and PP filled with different amounts of synthesized  $\text{TiO}_2$ .

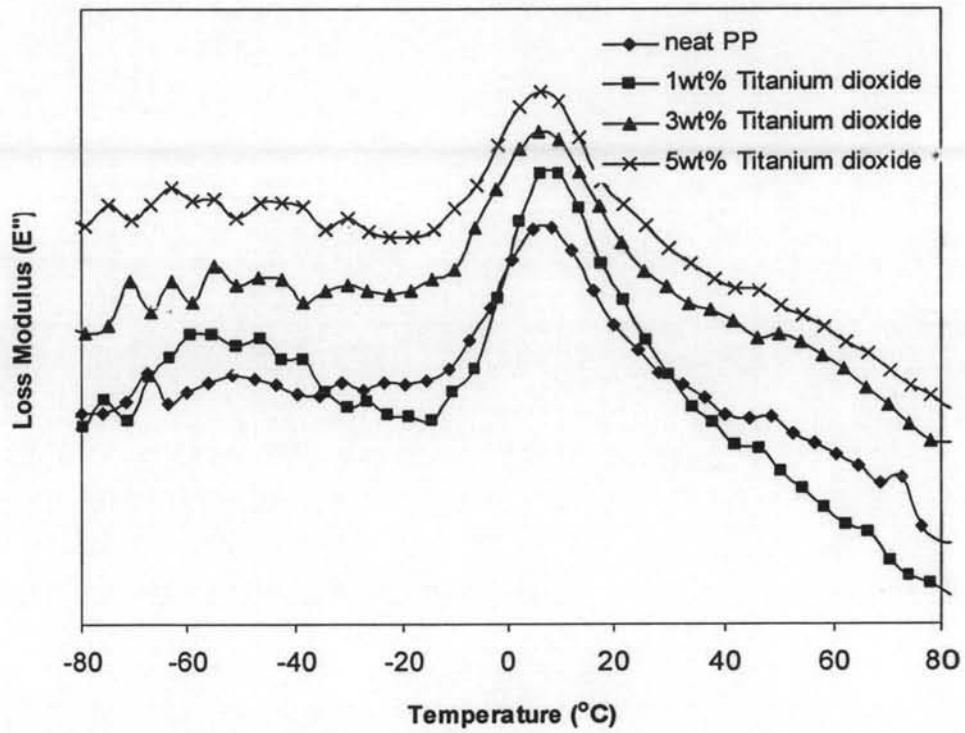
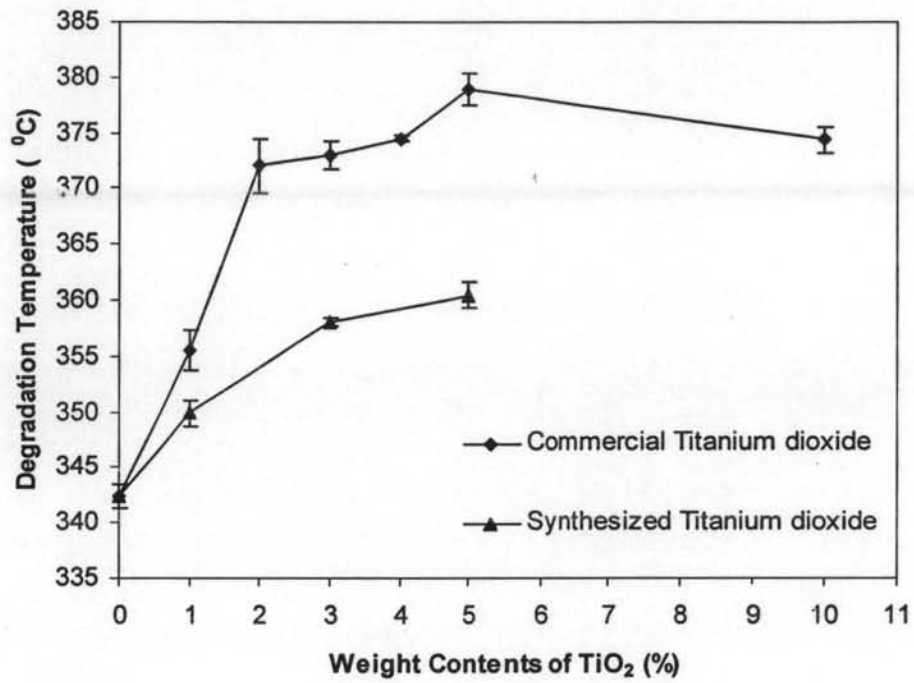
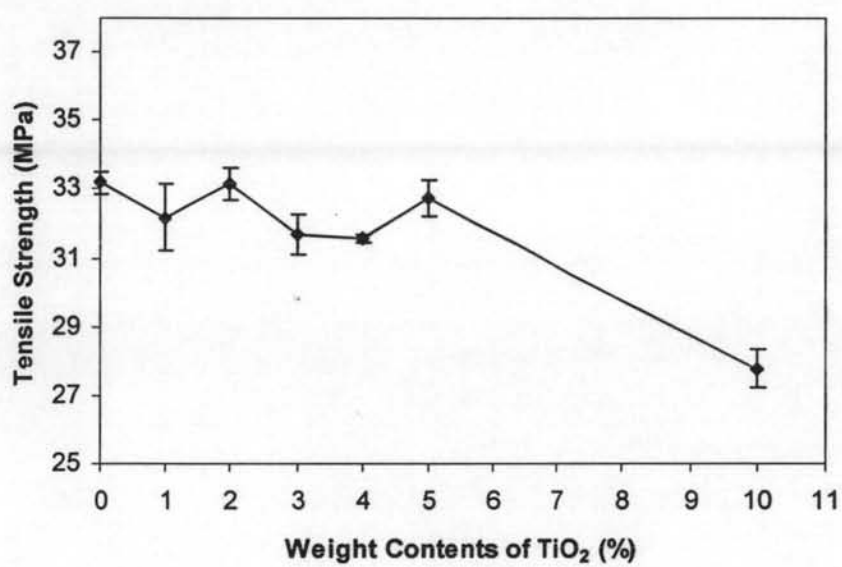


Figure 4.11 Degradation Temperature for all PP composites prepared.





**Figure 4.12** Tensile strength for neat PP and PP composites with different amounts of commercial  $\text{TiO}_2$ .



**Figure 4.13** Percentage of elongation for neat PP and PP composites with different amounts of commercial  $\text{TiO}_2$ .

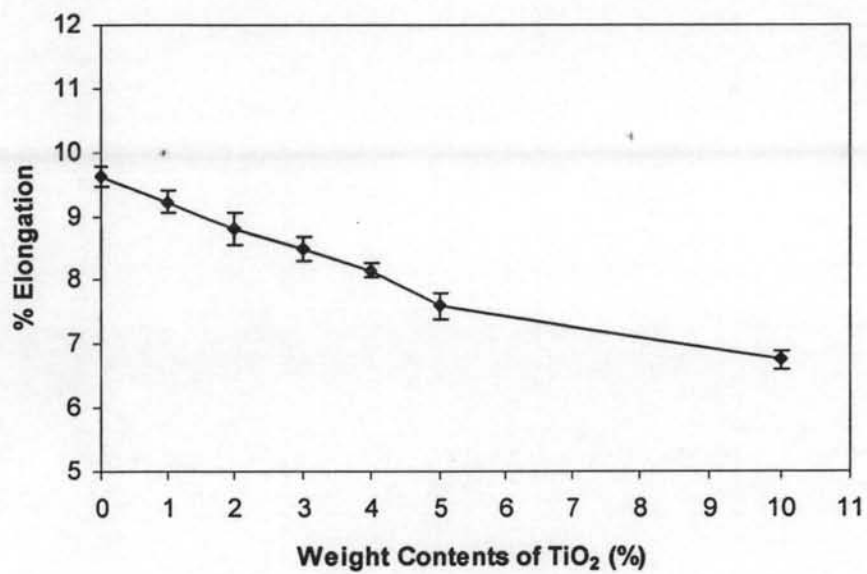


**Figure 4.14** Young's modulus for neat PP and PP composites with different amounts of commercial  $\text{TiO}_2$ .

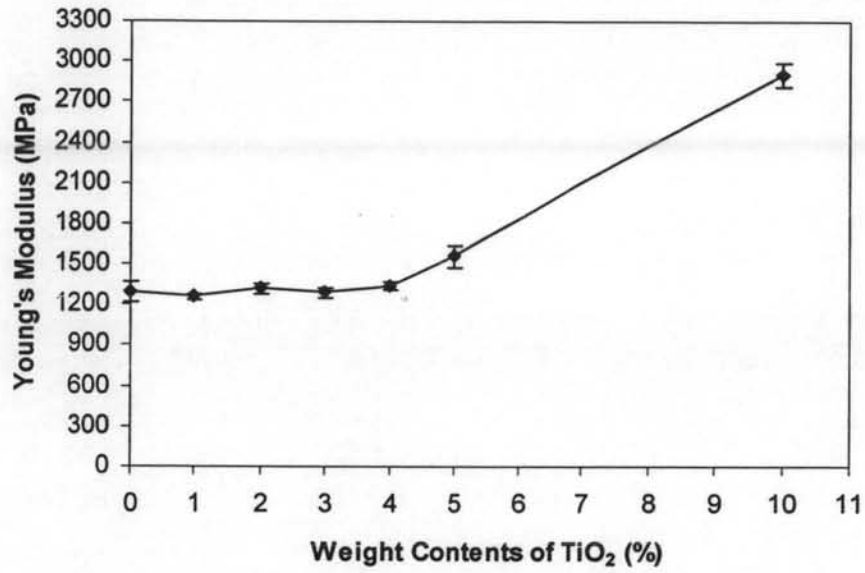


**Figure 4.15** Tensile strength for neat PP and PP composites with different amounts of synthesized TiO<sub>2</sub>.

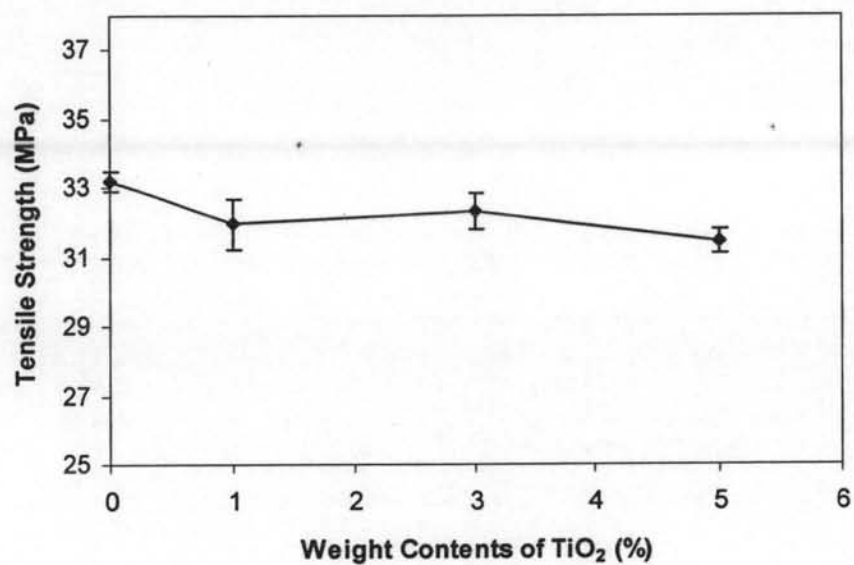


**Figure 4.16** Percentage of elongation for neat PP and PP composites with different amounts of synthesized  $\text{TiO}_2$ .

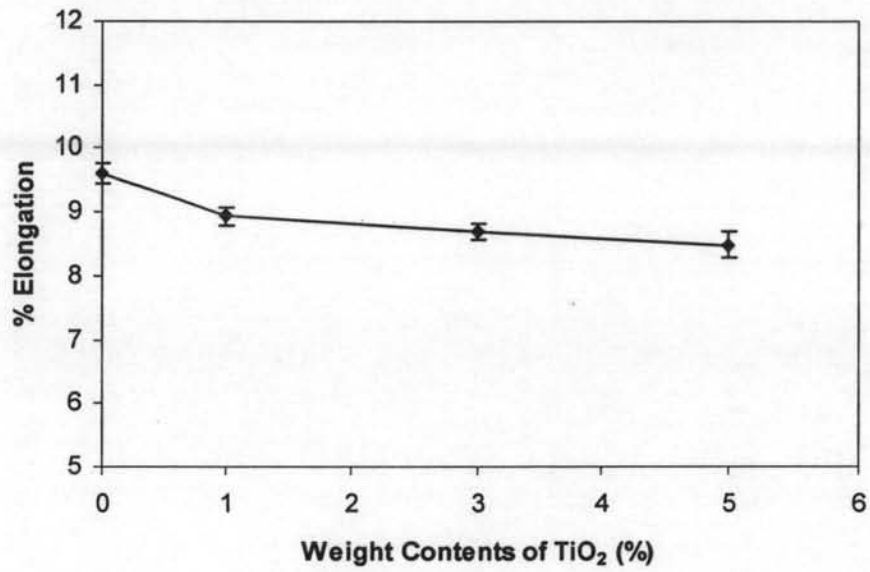


**Figure 4.17** Young's modulus for neat PP and PP composites with different amounts of synthesized  $\text{TiO}_2$ .

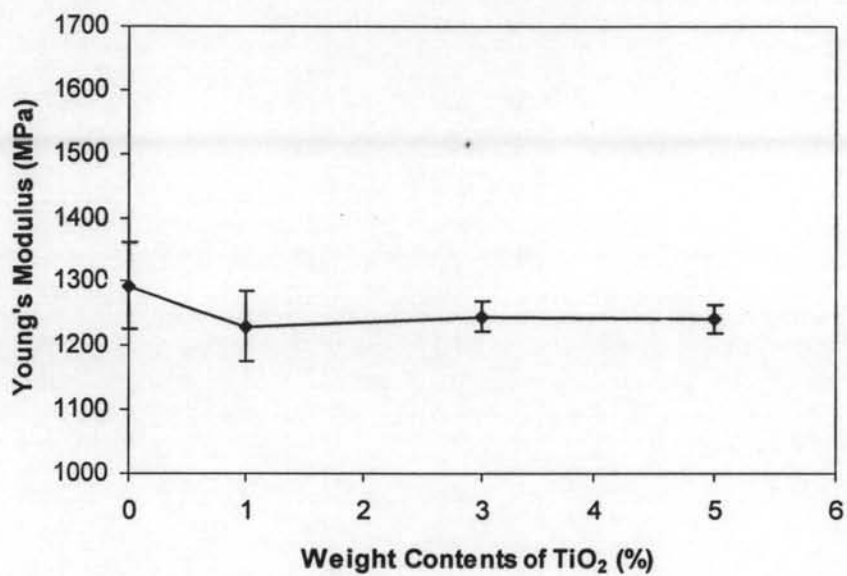
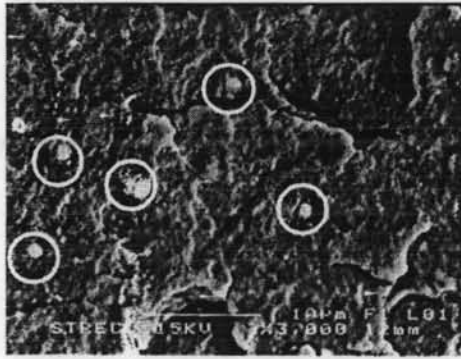
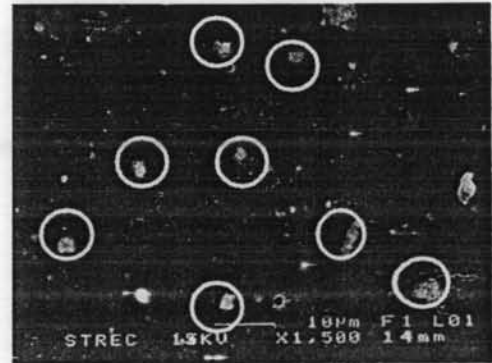


**Figure 4.18** SEM micrographs of fractured surfaces of PP nanocomposites with average particle size and standard deviation: (a) 5wt% commercial  $\text{TiO}_2$  and (b) 10wt% commercial  $\text{TiO}_2$ .



(a) 752 nm SD 229



(b) 2161 nm SD 484



**Table 4.1** Characteristics of non isothermal melt crystallization and subsequent melting behavior observed for PP and PP filled with different amounts of commercial TiO<sub>2</sub>

Samples	T <sub>c</sub> (°C)	T <sub>c</sub> (onset) (°C)	T <sub>m</sub> (°C)	T <sub>m</sub> (onset) (°C)	ΔH <sub>m</sub> (J/g)
PP	112.63	115.24	163.03	157.32	74.33
1wt% TiO <sub>2</sub>	112.80	116.45	161.86	157.21	80.86
2wt% TiO <sub>2</sub>	112.80	116.37	163.86	156.86	78.25
3wt% TiO <sub>2</sub>	113.63	118.71	161.70	157.40	81.63
4wt% TiO <sub>2</sub>	114.80	120.57	162.53	157.09	86.28
5wt% TiO <sub>2</sub>	118.80	121.54	164.03	158.19	87.23
10wt%TiO <sub>2</sub>	120.13	124.17	164.20	157.93	101.16

**Table 4.2** Characteristics of non isothermal melt crystallization and subsequent melting behavior observed for PP and PP filled with different amounts of synthesized TiO<sub>2</sub>

Samples	T <sub>c</sub> (°C)	T <sub>c</sub> (onset) (°C)	T <sub>m</sub> (°C)	T <sub>m</sub> (onset) (°C)	ΔH <sub>m</sub> (J/g)
PP	112.63	115.24	163.03	157.32	74.33
1wt% TiO <sub>2</sub>	111.63	114.98	162.70	156.68	80.66
3wt% TiO <sub>2</sub>	112.13	115.10	162.37	156.50	78.06
5wt% TiO <sub>2</sub>	112.30	115.70	163.70	156.79	78.19

**Table 4.3** The degree of crystallinity of neat PP and PP filled with different amounts of both commercial and synthesized TiO<sub>2</sub>

Samples	Degree of crystallinity (%)
PP	57.55
1wt% commercial TiO <sub>2</sub>	56.67
2wt% commercial TiO <sub>2</sub>	56.11
3wt% commercial TiO <sub>2</sub>	57.71
4wt% commercial TiO <sub>2</sub>	58.52
5wt% commercial TiO <sub>2</sub>	60.96
10wt% commercial TiO <sub>2</sub>	64.13
1wt% synthesized TiO <sub>2</sub>	57.56
3wt% synthesized TiO <sub>2</sub>	57.62
5wt% synthesized TiO <sub>2</sub>	58.36